Aggregation-Induced Emission of Precursors to Porous Molecular Crystals

Zhenglin Zhang, Mohamed I. Hashim and Ognjen Š. Miljanić*
Department of Chemistry, University of Houston, 112 Fleming Building, Houston, Texas 77204-5003, United States
Email: miljanic@uh.edu Phone: +1.832.842.8827 Web: www.miljanicgroup.com

Supporting Information

General Methods and Materials

Schlenk flasks or vials with PTFE/Liner caps were used as reaction vessels for the synthesis of precursors, while standard scintillation bottles were used as vessels for the synthesis of compound **1**. Column chromatography was carried out on silica gel 60, 32–63 mesh and basic aluminum oxide Act. 1, 50–200 μm (Sorbent Technologies). Analytical TLC was performed on J. T. Baker plastic-backed silica gel IB-F plates and aluminum oxide IB-F plates. The ^{1}H and ^{19}F NMR spectra were recorded on JEOL ECA-600, ECA-500, or ECX-400P spectrometers using the peaks of tetramethylsilane or residual solvent as standards. Trifluorotoluene ($PhCF_3$, δ = −63.72 ppm) was used as the internal standard in ^{19}F NMR spectra. ^{13}C NMR spectra were not included since they are not informative, due to the poor solubility of the prepared compounds and extensive coupling between ^{13}C and ^{19}F nuclei; low intensities and many missing peaks were observed. Analytical thin-layer chromatography was performed on Fluka silica gel/TLC plates with a fluorescent indicator that emitted when irradiated at 254 nm.

All reactions were performed under nitrogen atmosphere in oven-dried glassware. The following starting materials and solvents were obtained from the respective commercial sources and used without further purification: Boc_2O (Alfa Aesar); triphenylchloromethane (TrCl, AK Scientific); *N*,*N*-dimethylacetamide (DMA), *N*,*N*-dimethylformamide (DMF), and potassium *t*-butoxide (*t*-BuOK) (Sigma Aldrich); 2,3,5,6-tetrafluorobenzene (Synquest); triethylamine (Et_3N), tetrakis(triphenylphosphine)palladium(0) ($Pd(PPh_3)_4$), 4-iodopyrazole and trifluoroacetic acid (TFA) (Matrix Scientific); methanol, ethanol, dichloromethane, chloroform, (Sigma Aldrich); water (Milli-Q, deionized). Compound **2** was prepared as previously reported.

Experiments are presented in the order following the discussion of the manuscript.
Compound numbers are identical to those in the main text of the manuscript.

Synthesis of Compound 1

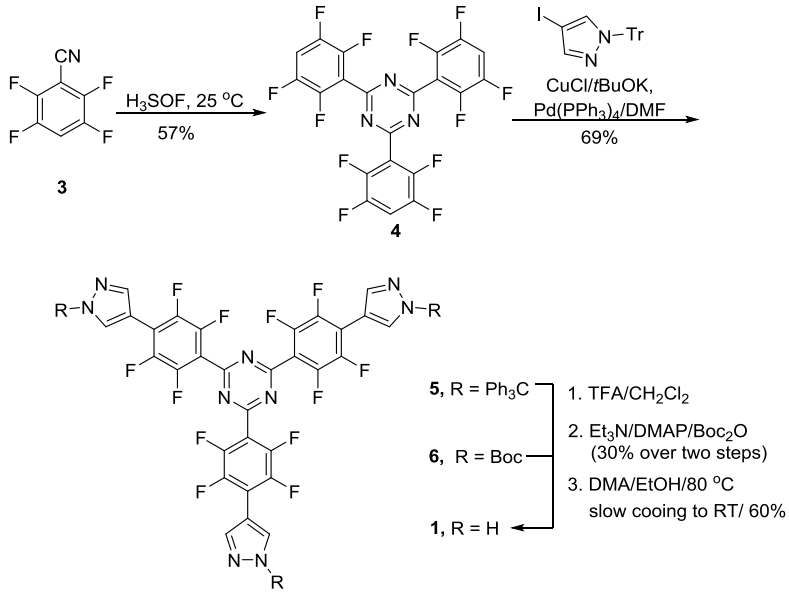

Synthesis of 2,4,6-tris(2,3,5,6-tetrafluorophenyl)-1,3,5-triazine (**4**): Compound 2,3,5,6 -tetrafluorobenzonitrile[1] (6.00 g, 34 mmol) and fluorosulfuric acid (5.6 mL, 103 mmol) were placed in a 20 mL Schlenk flask with stirring at room temperature for 3 d. The mixture was poured into cold water with ice (30 mL) and the precipitated solid was collected, washed with H_2O until neutral, EtOH (15 mL), and Et_2O (2 × 5 mL) and air dried for 12 hours. This yielded 3.39 g (57%) of a white powder solid, mp 229–230 °C. ^{1}H NMR (600 MHz, DMSO-d_6): δ 8.23–8.29 (m, 3H) ppm. ^{19}F NMR (564 MHz, DMSO-d_6): δ –137.76 to –137.83 (m, 6F), –141.73 to –141.77 (m, 6F) ppm. FT-IR (neat): ῡ 3059, 1525, 1501, 1481, 1461, 1391, 1346, 1239, 1270, 1189, 1174, 1002, 935, 867, 840, 735, 715 698, 664, 565 cm^{-1}. ESI MS *m/z*: 526 (100 %), 441 (10 %), 417 (20 %), 401 (5 %).

Synthesis of 2,4,6-tris(2,3,5,6-tetrafluoro-4-(1-trityl-1H-pyrazol-4-yl)phenyl)-1,3,5-triazine (**5**): A 100 mL screw cap pressure vessel was equipped with a magnetic stir bar and charged with CuCl (1.68 g, 17 mmol) and *t*-BuOK (1.91 g, 17 mmol) inside the glovebox. Dry DMF (20 mL) was added, and the vessel was sealed and vigorously stirred at 25 °C for 1 h. Next, 2,4,6-tris(2,3,5,6-tetrafluorophenyl)-1,3,5-triazine (2.63 g, 5 mmol) was added in one portion and then the reaction mixture was vigorously stirred at 25 °C for 1 h. Catalyst $Pd(PPh_3)_4$ (174 mg, 0.15 mmol) was added, followed by 4-iodo-1-trityl-1H-pyrazole (8.73 g, 20 mmol). The reaction vessel was sealed, taken out of the glovebox and placed inside an oil bath preheated to 100 °C, where it was stirred vigorously for

22 h. The reaction mixture was cooled to 25 °C, diluted with DCM (400 mL) and poured into a beaker that contained 100 mL NH_4OH (aq), eight spatula scoops of NH_4Cl(s) and 300 mL of deionized H_2O. This mixture was stirred in the beaker for 30 min. The blue aqueous layer was poured out and the organic layer was filter out through a celite pad, dried with $MgSO_4$ and was dry-absorbed on silica gel. After purification by column chromatography on silica gel (using hexanes/CH_2Cl_2 as eluent) and evaporation of the fractions containing the product, compound **5** was obtained (5.00 g, 69%). ^{1}H NMR (400 MHz, $CDCl_3$): δ 8.25 (s, 3H), 8.04 (s, 3H), 7.37–7.35 (m, 27H), 7.23–7.20 (m, 15H) ppm. ^{19}F NMR (376 MHz, $CDCl_3$): δ –139.87 to –139.96 (m, 6F), –142.00 to –142.08 (m, 6F) ppm.

Synthesis of tri-tert-butyl 4,4',4''-((1,3,5-triazine-2,4,6-triyl)tris(2,3,5,6-tetrafluorobenzene-4,1-diyl))tris(1H-pyrazole-1-carboxylate) (**6**): Compound 2,4,6-tris(2,3,5,6-tetrafluoro-4-(1-trityl-1H-pyrazol-4-yl)phenyl)-1,3,5-triazine (6.60 g, 4.55 mmol) was dissolved in 100 mL of DCM in a 250 mL round bottom flask equipped with a magnetic stir bar. The following clear solution was stirred vigorously, then TFA (10 mL, 131 mmol) was added resulting in a green solution. Stirring was continued for 24 h at 25 °C. The resulting salt that precipitated was filtered off and washed with fresh DCM (3 × 50 mL). Resulting tan solid was then vacuum dried for 3 h. A 250 mL round bottom flask equipped with a magnetic stir bar was charged with the crude isolated salt (3.4 g, 4.70 mmol) and 70 mL of DCM. This suspension was cooled to 0 °C followed by the slow addition of NEt_3 (6 mL, 81 mmol) over 10 min. This reaction mixture was allowed to stir and maintained at a temperature of 0 °C for another 10 min and then the ice bath was removed, followed by the addition of dimethylaminopyridine (0.38 g, 3 mmol), and finally di-*tert*-butyl dicarbonate (7.00 g, 33 mmol) was added to the reaction mixture. The round bottom flask was then sealed with a septum and connected to a bubbler in order to visually monitor the evolution of CO_2 gas. The reaction mixture was stirred vigorously at 25 °C until the evolution of CO_2 ceased (~24 h). Upon completion, the reaction mixture was dry-absorbed on silica gel. After purification by column chromatography on silica gel (using hexanes/EtOAc as eluent) and evaporation of the fractions containing the product was obtained as a yellowish solid (1.40 g, 30% over two steps). Mp: >350 °C (decomp). ^{1}H NMR (400 MHz, $CDCl_3$): δ 8.60 (s, 3H), 8.20 (s, 3H), 1.69 (s, 30H) ppm. ^{19}F NMR (376 MHz, $CDCl_3$): δ –138.97 to –139.05 (m, 6F), –141.04 to –141.13 (m, 6F) ppm. FT-IR (neat): ῡ 2982, 2360, 1794,

1758, 1643, 1566, 1522, 1475, 1372, 1357, 1340, 1288, 1259, 1233, 1214, 1145, 1038, 965, 874, 839, 812, 751, 743, 707, 672, 657, 636, 596, 513 cm^{-1}.

Compound **1**: Tri-*tert*-butyl 4,4',4''-((1,3,5-triazine-2,4,6-triyl)tris(2,3,5,6-tetrafluorobenzene-4,1-diyl))tris(1H-pyrazole-1-carboxylate) (100 mg, 0.098 mmol) was added to a 20 mL scintillation vial. Solvents DMA (10 mL) and EtOH (10 mL) were added to the solid and the bottle was capped. The vial was sonicated for 10 min and then sealed and placed into a variable temperature oven. The oven was programmed to heat the sample at 80 °C for 1 d and then to slowly cool it to room temperature by ~4 °C/h. The resulting colourless needle crystals (43 mg, 60 %) were washed with EtOH and air-dried. Mp: >350 °C (decomp). ^{1}H NMR (600 MHz, $CDCl_3$): δ 13.53 (s, 3H), 8.36 (s, 3H), 8.02 (s, 30H). ^{19}F NMR (564 MHz, $CDCl_3$): δ –138.97 to –139.05 (m, 6F), –141.04 to –141.13 (m, 6F). FT-IR (neat): ῡ 3147, 2827, 1648, 1514, 1471, 1407, 1364, 1320, 1257, 1207, 1175, 1032, 989, 964, 947, 871, 865, 831, 811, 705, 658, 609, 457 cm^{-1}.

^{1}H and ^{19}F NMR Spectra of Starting Materials

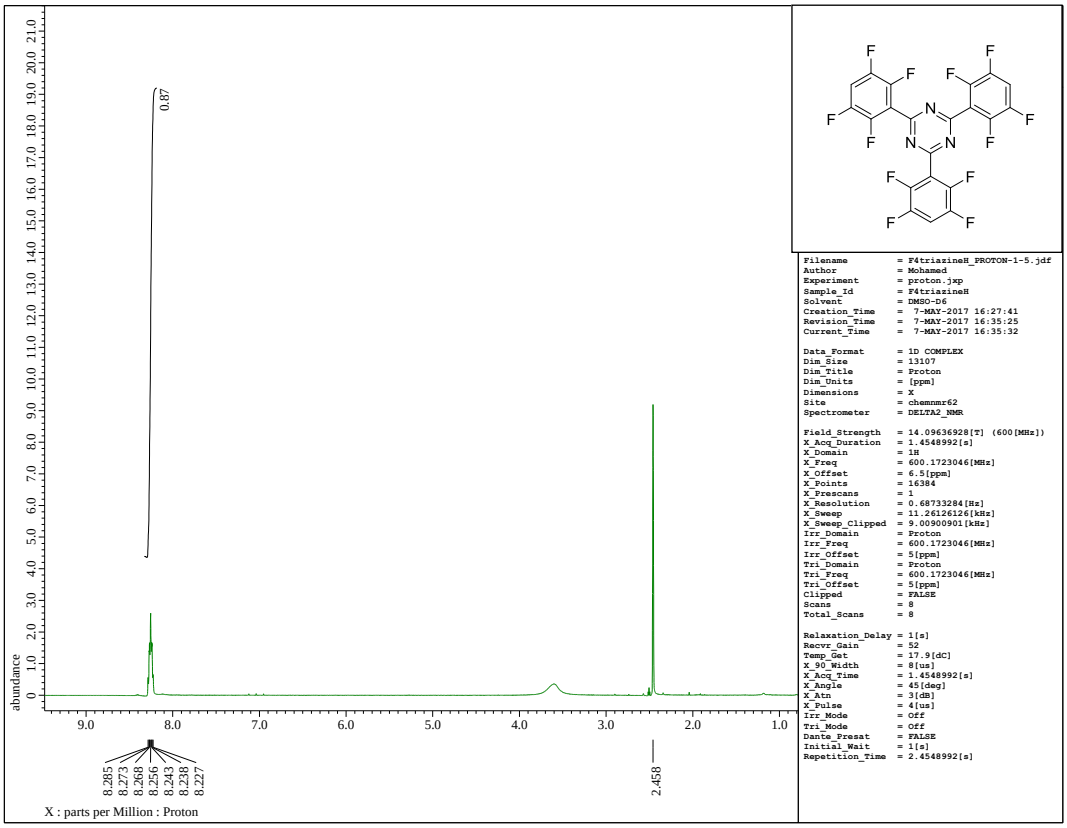

Figure 1. ^{1}H Spectrum of compound **4**.

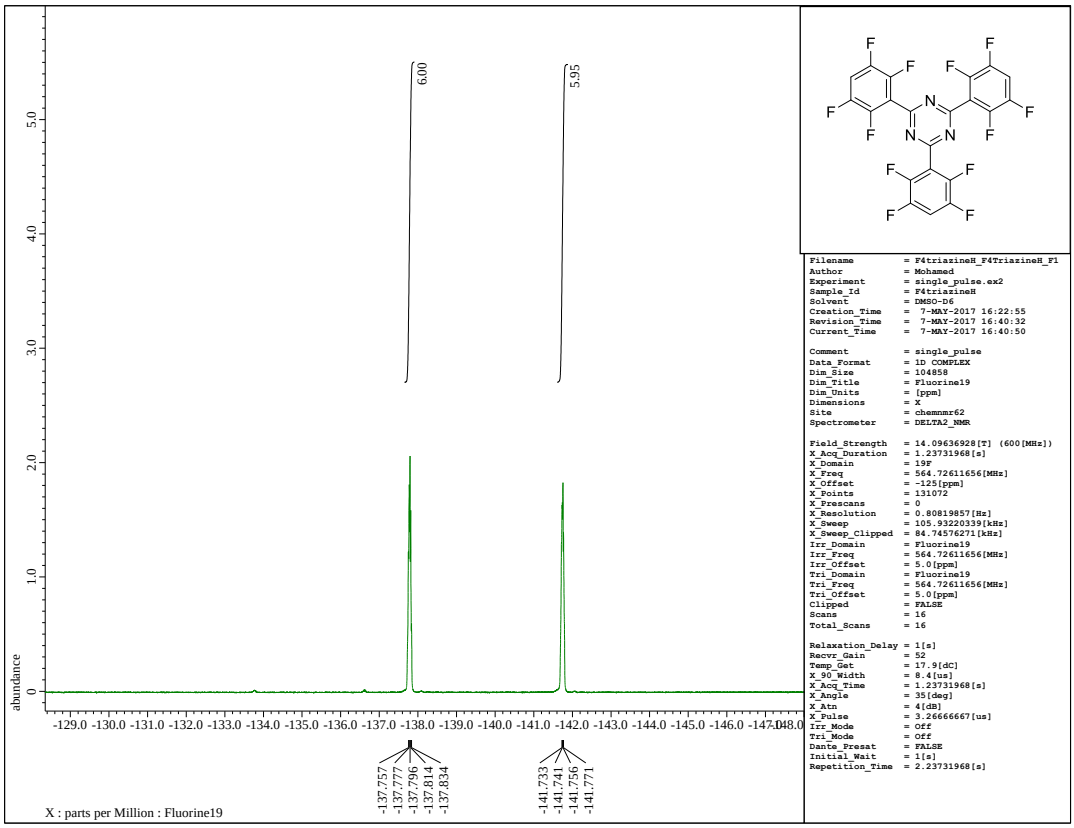

Figure 2. ^{19}F Spectrum of compound **4**.

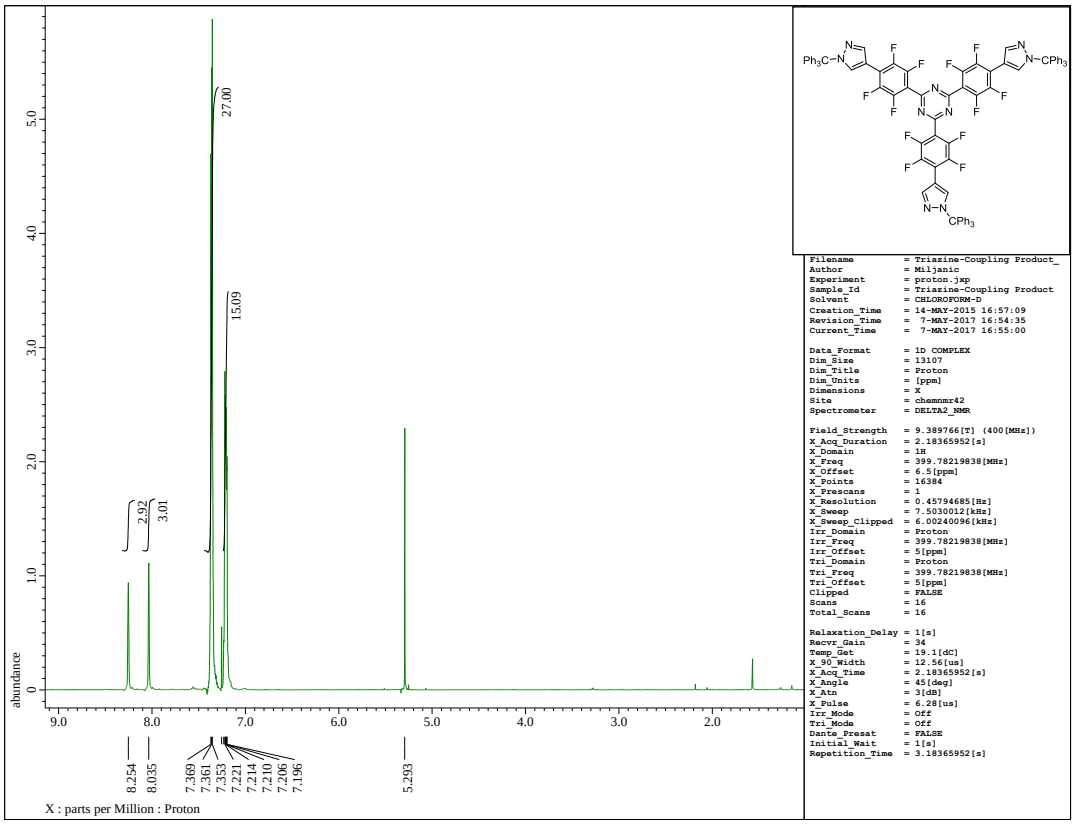

Figure 3. ^{1}H Spectrum of compound **5**.

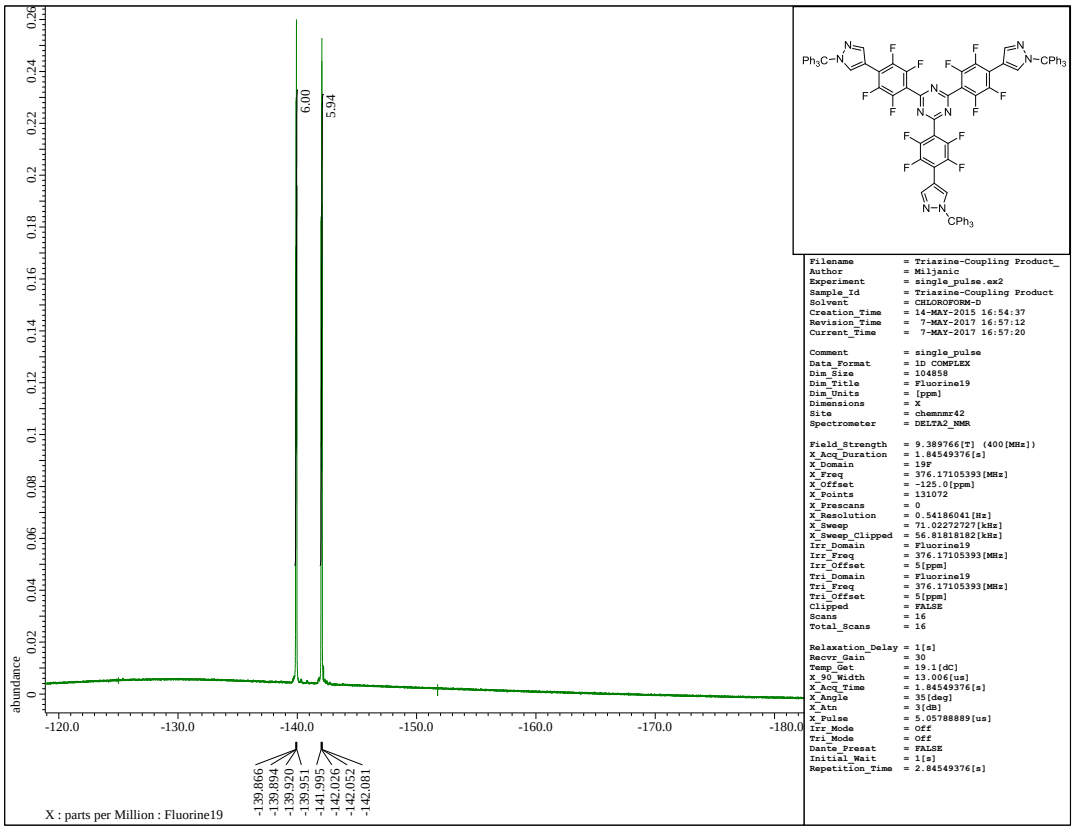

Figure 4. ^{19}F Spectrum of compound **5**.

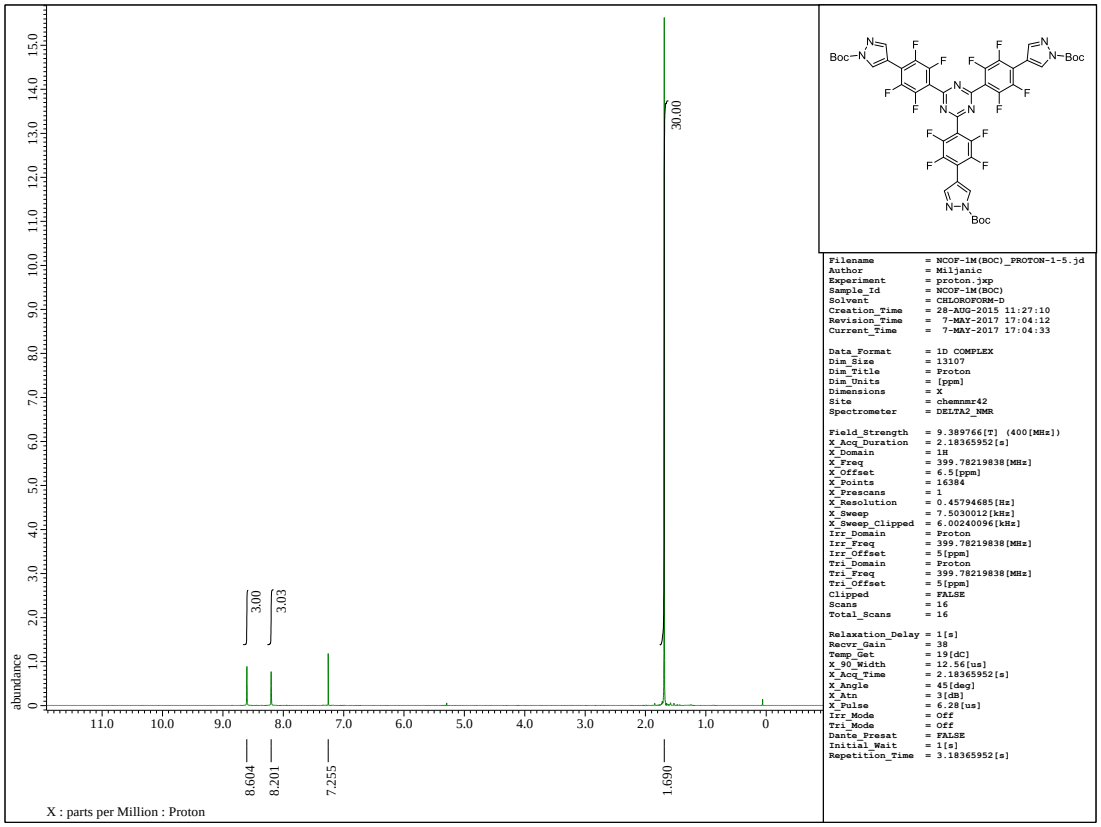

Figure 5. ^{1}H Spectrum of compound **6**.

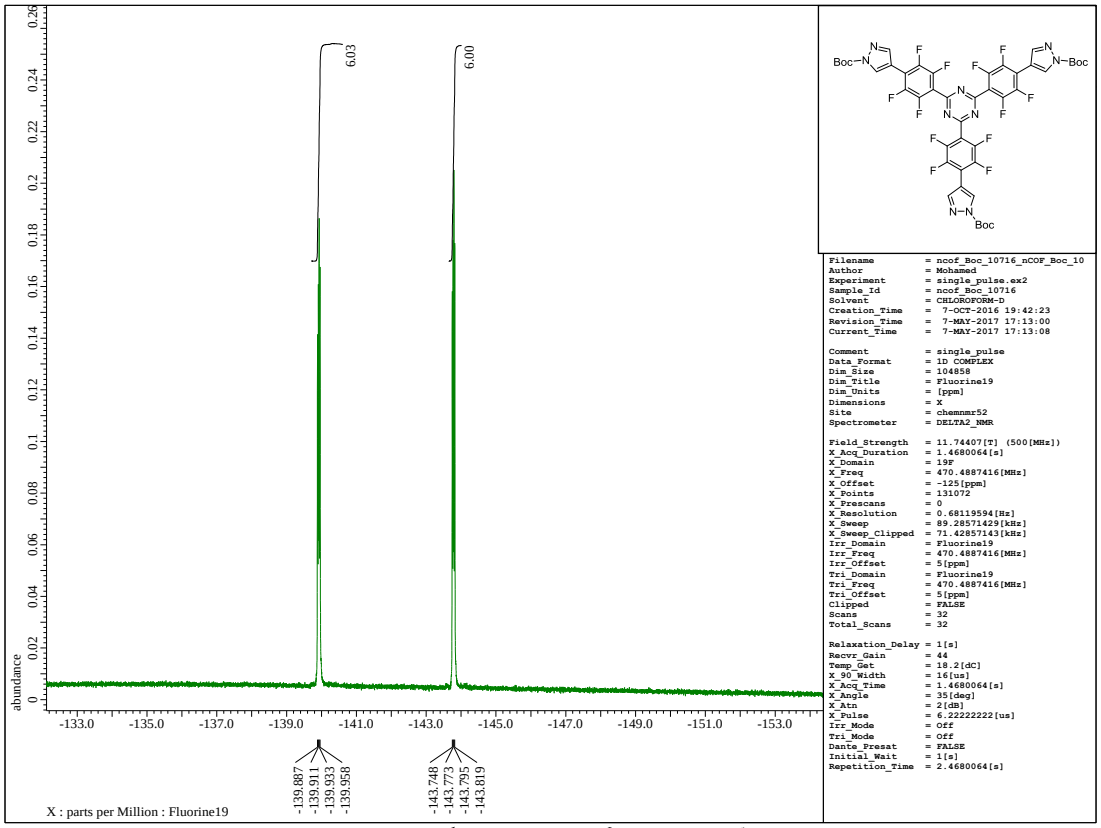

Figure 6. ^{1}H Spectra of compound **6**.

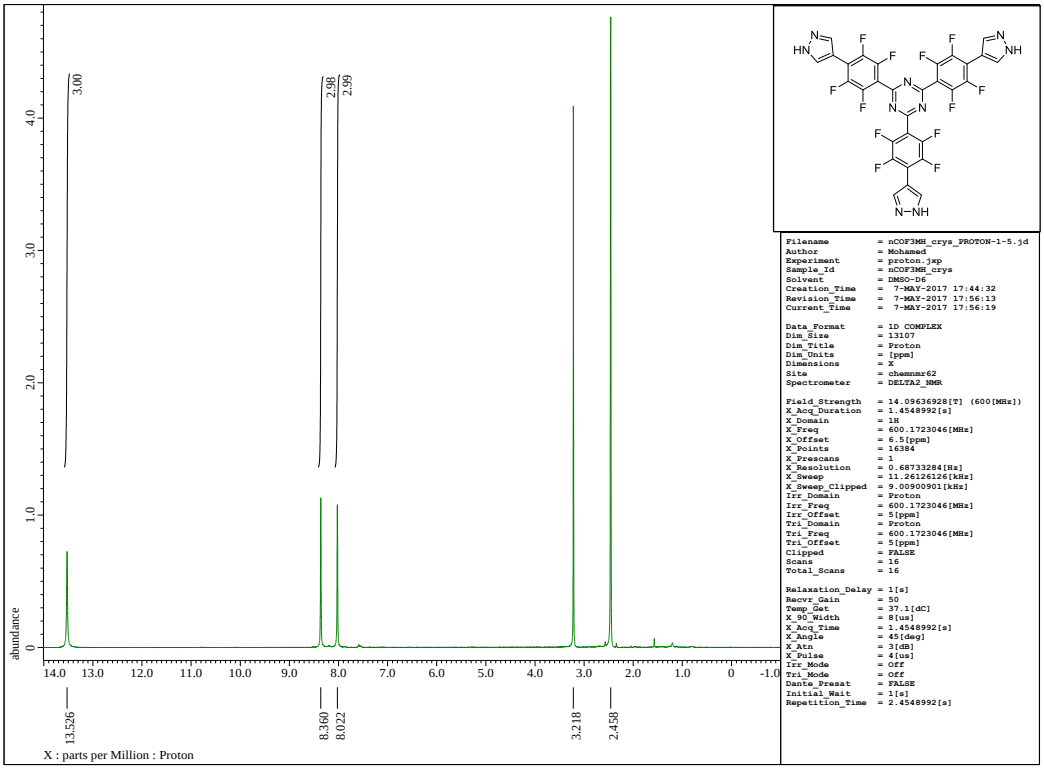

Figure 7. ^{1}H Spectrum of compound **1**.

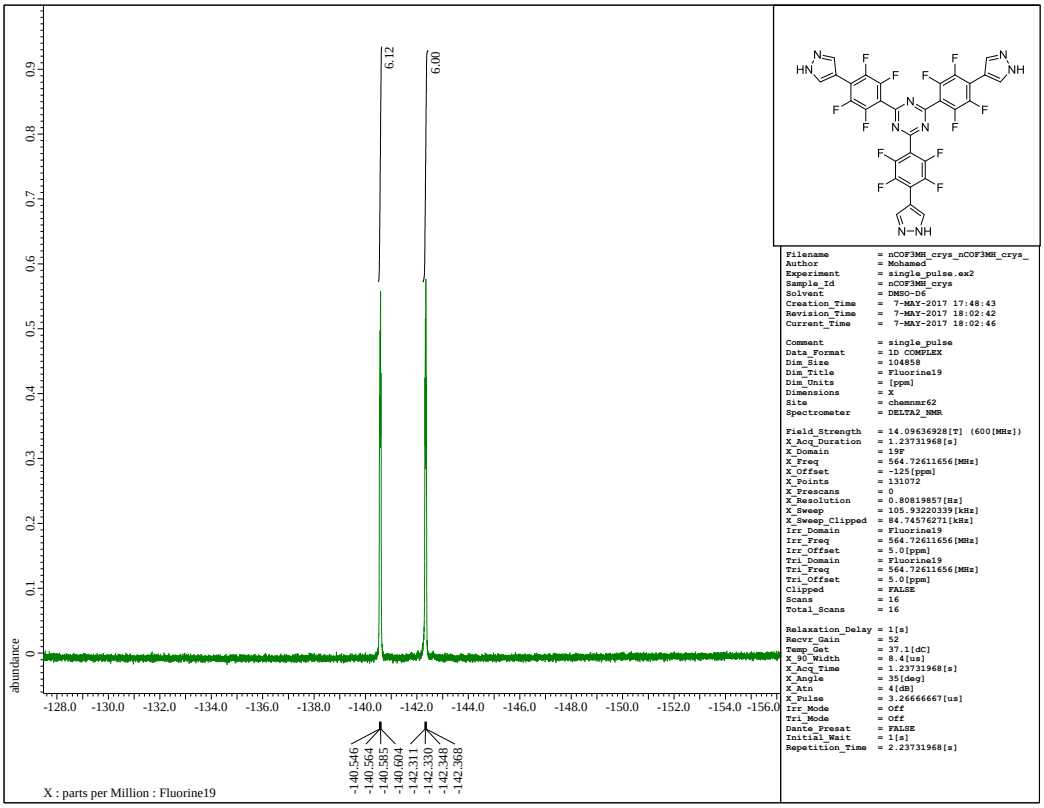

Figure 8. ^{19}F Spectrum of compound **1**.

X-ray Crystallographic Analysis of Compound 1

All measurements were performed by Dr. Xiqu Wang (UH) using a Bruker DUO platform diffractometer equipped with a 4K CCD APEX II detector and an Incoatec 30 Watt Cu microsource with compact multilayer optics. A hemisphere of data (2713 frames at 4 cm detector distance) was collected using a narrow-frame algorithm with scan widths of 0.50 % in omega and an exposure time of 25 s/frame. The data were integrated using the Bruker-Nonius SAINT program, with the intensities corrected for Lorentz factor, polarization, air absorption, and absorption due to variation in the path length through the detector faceplate. The data were scaled, and an absorption correction was applied using SADABS. Redundant reflections were averaged. Final cell constants were refined using 7541 reflections having $I>10\sigma(I)$. All of the solvent sites are heavily disordered, and the identities of some solvent species are impossible to determine precisely. Most of the solvent identities and occupancies in this model are just estimates, and should not be relied on too much. They represent just one possibility out of many. Some of the solvent sites are not fully occupied, either due to some loss during crystal handling or because the disorder is so severe that some solvent locations cannot be identified. It is also quite possible that some heavily disordered water has been omitted.

Crystal Data and Structure Refinement Parameters for Compound **1**

Empirical formula	$C_{32.42}H_9F_{12}N_{9.35}O_{1.38}$	
Formula weight	779.57	
Temperature	100(2) K	
Wavelength	1.54178 Å	
Crystal system	Monoclinic	
Space group	*C*2/c	
Unit cell dimensions	a = 19.1610(7) Å	$\alpha = 90°$
	b = 34.1885(15) Å	$\beta = 110.374(3)°$
	c = 7.1304(4) Å	$\gamma = 90°$
Volume	4378.8(4) Å^3	
Z	4	
Density (calculated)	1.183 Mg/m^3	
Crystal size	0.18 x 0.14 x 0.11 mm^3	
Reflections collected	15731	
Independent reflections	3937 [R(int) = 0.0427]	
Refinement method	Full-matrix least-squares on F^2	
Data / restraints / parameters	3937 / 15 / 260	

Goodness-of-fit on F^2	1.020
Final R indices $[I>2\sigma(I)]$	$R_1 = 0.0726$, w$R_2 = 0.2396$
R indices (all data)	$R_1 = 0.0884$, w$R_2 = 0.2592$
Largest diff. peak and hole	0.617 and –0.456 e/Å^{-3}

UV/Vis Spectroscopic Experiments

DMF and H_2O of spectrophotometric grade were used in all spectral experiments. The crystals of compound **1** or compound **2** were dissolved in DMF with heating to facilitate complete dissolution of the sample. These samples were then used in the preparation of a 500 μM stock solution. Then, a 0.06 mL sample of the stock solution was diluted to 3 mL with a specified volume of DMF and H_2O under vigorous stirring yielding a final concentration of 10 μM. The water content was changed from 0 to 98% by volume. Absorption spectra were recorded using a PerkinElmer LAMBDA 25 UV/VIS spectrometer, and the steady-state emission spectra were measured by a Horiba FluoroMax-4 spectrofluorometer. The solid-state excitation and emission spectra were measured by PTI QuantaMaster QM4 CW spectrofluorometer.

Theoretical Calculations

Structure optimizations were carried out with the B3LYP density functional and 6-31G(d) basis set as implemented in the Gaussian 09 program package. Rigid scans of potential energy along the C9–C12 bond of the optimized structures were performed with the same conditions as the structures' optimization.

Optimized Cartesian Coordinates for Compound **1**

Atom	X	Y	Z
C1	−7.469816	−3.149044	0.308842
H2	−7.710563	−2.270936	0.886171
C3	−6.212166	−3.512866	−0.264658
C4	−6.481129	−4.728984	−0.894511
H5	−5.852371	−5.39605	−1.460003
C6	−4.939418	−2.795074	−0.214482
C7	−4.764801	−1.608369	0.516962
C8	−3.557851	−0.920656	0.560862
C9	−2.422182	−1.380109	−0.120591
C10	−2.578999	−2.565837	−0.851454
C11	−3.793084	−3.237716	−0.896145
C12	−1.132374	−0.652628	−0.065593
C13	0.009493	1.295452	0.000863
C14	0.020424	2.776614	−0.000528
C15	1.018287	3.510393	−0.65722
C16	1.020161	4.900132	−0.66133
C17	0.041428	5.665428	−0.005503
C18	0.050878	7.127419	−0.004866
C19	1.028882	8.017441	−0.547396
H20	1.945524	7.769801	−1.058201
F21	−5.786255	−1.093696	1.227423
F22	−3.502424	0.178634	1.319089
F23	−1.569813	−3.065621	−1.572512
F24	−3.845471	−4.358149	−1.646153
F25	1.981718	2.891656	−1.346524
F26	2.010181	5.506678	−1.343413
N27	−8.414637	−4.045017	0.058841
N28	−7.785178	−4.993505	−0.67182
H29	−8.311433	−5.795411	−0.985945
N30	0.708958	9.290492	−0.360701
N31	−1.179589	0.685926	−0.096524
N32	−0.010609	−1.382479	0.001919
C33	7.381445	−3.235489	−0.303842
H34	7.671592	−2.374482	−0.882282
C35	6.161847	−3.599534	0.268893

C36	6.449796	−4.848952	0.900547
H37	5.781116	−5.48269	1.460544
C38	4.897997	−2.865957	0.222596
C39	4.738732	−1.676193	−0.507959
C40	3.5438	−0.970697	−0.555437
C41	2.401089	−1.415589	0.124747
C42	2.54154	−2.603233	0.855243
C43	3.746201	−3.294351	0.903529
C44	1.121981	−0.669558	0.069415
C45	−0.967791	3.525869	0.65404
C46	−0.947659	4.914158	0.651713
C47	−0.90709	7.986527	0.535716
H48	−1.833401	7.792237	1.04994
F49	5.772922	−1.176871	−1.21587
F50	3.505357	0.129428	−1.313864
F51	1.524475	−3.088709	1.574442
F52	3.778486	−4.412121	1.653915
F53	−1.940432	2.923512	1.345169
F54	−1.930315	5.541745	1.330458
N55	8.25429	−4.217936	0.001372
H56	9.228539	−4.27553	−0.25592
N57	7.712556	−5.217301	0.734588
N58	−0.472021	9.241094	0.297095
H59	−0.923178	10.106673	0.553816
N60	1.189168	0.668218	0.099191

Rigid scans of potential energy along the C9–C12 of the optimized structures of compound **1**

Dihedral angle C10–C9–C12–N32 (°)	Total Energy (kcal mol^{-1})
1.48955	−1781667.924
11.48955	−1781668.235
21.48955	−1781669.055
31.48955	−1781669.826
41.48955	−1781670.046
51.48955	−1781669.796
61.48955	−1781669.199
71.48955	−1781668.598
81.48955	−1781668.208
91.48955	−1781668.107
101.48955	−1781668.354
111.48955	−1781668.871
121.48955	−1781669.579
131.48955	−1781670.176
141.48955	−1781670.422
151.48955	−1781670.098
161.48955	−1781669.247

171.48955	−1781668.326
181.48955	−1781667.883
191.48955	−1781668.197
201.48955	−1781669.043
211.48955	−1781669.773
221.48955	−1781670.026
231.48955	−1781669.723
241.48955	−1781669.145
251.48955	−1781668.571
261.48955	−1781668.183
271.48955	−1781668.105
281.48955	−1781668.343
291.48955	−1781668.866
301.48955	−1781669.579
311.48955	−1781670.219
321.48955	−1781670.462
331.48955	−1781670.143
341.48955	−1781669.289
351.48955	−1781668.37
361.48955	−1781667.924

Optimized Cartesian Coordinates for Compound **2**

Atom	X	Y	Z
C1	−0.972931	8.094919	−0.734778
H2	−0.154899	8.072789	−1.435141
C3	−1.592766	7.083117	−0.001129
C4	−2.603106	7.775888	0.734297
H5	−3.318379	7.368811	1.430814
C6	−1.272612	5.655229	0.002501
C7	−0.251366	5.102707	−0.787594
C8	0.054249	3.748356	−0.789245
C9	−0.633723	2.821293	0.004537
C10	−1.652554	3.365859	0.796577
C11	−1.959486	4.721266	0.794815
C12	−0.307966	1.372418	0.005217
C13	1.026199	0.94473	0.004866
H14	1.821508	1.677848	0.004688
C15	1.343933	−0.419873	0.00494
C16	0.30643	−1.361475	0.005175
H17	0.543715	−2.416802	0.005492
C18	−1.0342	−0.954359	0.00526
C19	−1.330817	0.41495	0.005482
H20	−2.363365	0.737197	0.006044
C21	2.761607	−0.862094	0.004067
C22	3.220687	−1.920915	−0.790299

C23	4.546429	−2.333298	−0.788774
C24	5.535306	−1.725812	0.002157
C25	5.069734	−0.664472	0.794992
C26	3.742446	−0.252693	0.796848
C27	6.931963	−2.16253	−0.00122
C28	7.497474	−3.207525	−0.732237
H29	7.068451	−3.906831	−1.430153
C30	8.03772	−1.632362	0.732124
H31	8.04373	−0.807345	1.426254
C32	−2.126409	−1.960563	0.004261
C33	−3.272568	−1.828002	−0.790503
C34	−4.293483	−2.768925	−0.788828
C35	−4.263022	−3.928892	0.002331
C36	−3.111372	−4.057112	0.795543
C37	−2.090106	−3.114599	0.797165
C38	−5.340336	−4.919243	−0.00121
C39	−6.521723	−4.892451	−0.742696
H40	−6.906152	−4.177703	−1.450904
C41	−5.441036	−6.135354	0.742139
H42	−4.735999	−6.546971	1.446379
N43	8.808714	−3.232241	−0.411407
H44	9.514032	−3.865031	−0.758639
N45	9.166799	−2.281277	0.480284
N46	−1.606746	9.242878	−0.413224
H47	−1.412707	10.169875	−0.761788
N48	−2.606803	9.077947	0.481378
N49	−7.202003	−6.012539	−0.417857
H50	−8.09969	−6.309728	−0.770423
N51	−6.565786	−6.790314	0.486523
F52	0.476873	5.896244	−1.600842
F53	1.045421	3.339926	−1.602789
F54	−2.373045	2.572897	1.610241
F55	−2.956651	5.12226	1.606651
F56	2.371757	−2.574438	−1.604726
F57	4.869736	−3.359997	−1.60291
F58	3.415764	0.767062	1.611312
F59	5.915442	−0.002034	1.607466
F60	−5.34413	−2.53454	−1.602871
F61	−3.412967	−0.766144	−1.605215
F62	−1.043806	−3.342477	1.611596
F63	−2.961622	−5.120581	1.608398

Rigid scans of potential energy along the C9–C12 of the optimized structures of compound **2**

Dihedral angle C10–C9–C12–C19(°)	Total Energy (kcal mol^{-1})
2.1806	−1751472.837
12.1806	−1751474.767
22.1806	−1751477.555
32.1806	−1751479.404
42.1806	−1751479.953
52.1806	−1751479.602
62.1806	−1751478.940
72.1806	−1751478.279
82.1806	−1751477.861
92.1806	−1751477.739
102.1806	−1751477.910
112.1806	−1751478.363
122.1806	−1751478.975
132.1806	−1751479.513
142.1806	−1751479.506
152.1806	−1751478.345
162.1806	−1751475.937
172.1806	−1751473.379
182.1806	−1751472.774
192.1806	−1751474.726
202.1806	−1751477.513
212.1806	−1751479.357
222.1806	−1751479.930
232.1806	−1751479.589
242.1806	−1751478.945
252.1806	−1751478.296
262.1806	−1751477.885
272.1806	−1751477.771
282.1806	−1751477.949
292.1806	−1751478.412
302.1806	−1751479.025
312.1806	−1751479.558
322.1806	−1751479.540
332.1806	−1751478.417
342.1806	−1751475.987
352.1806	−1751473.443
362.1806	−1751472.837

Variable Temperature ^{19}F NMR Studies

To evaluate intramolecular rotation and possible aggregation at low temperatures, we performed variable temperature ^{19}F NMR spectroscopic studies on **1** and **2**. To simplify the analysis, these studies were performed with simultaneous irradiation of one of the two peaks (labeled as **L** and **R** based on their position in the spectra), which caused decoupling and the other peak to appear as a singlet. All spectra were taken at concentrations of 0.3 mg mL^{-1} (for both **1** and **2**) in DMF-d_7. While all the peaks broaden at low temperature due to lowered solubility and possible aggregation, there is no significant difference in this behavior between compounds **1** and **2**, nor peaks **L** and **R**.

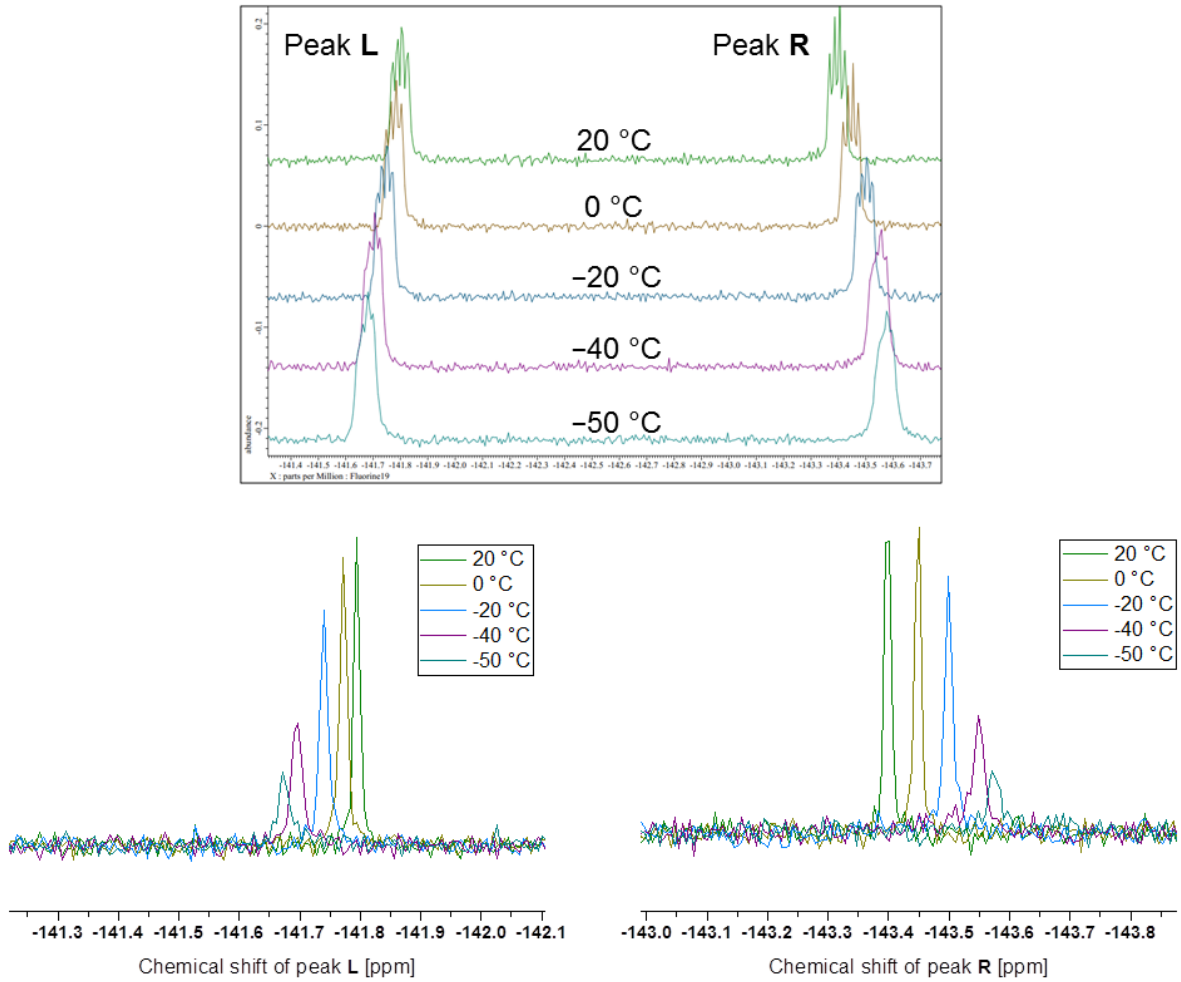

Figure 9. Variable temperature ^{19}F spectrum of compound **1**: comparison of spectra with the lowering of the temperature (top), and the shapes and positions of peaks L (bottom left) and R (bottom right) following decoupling.

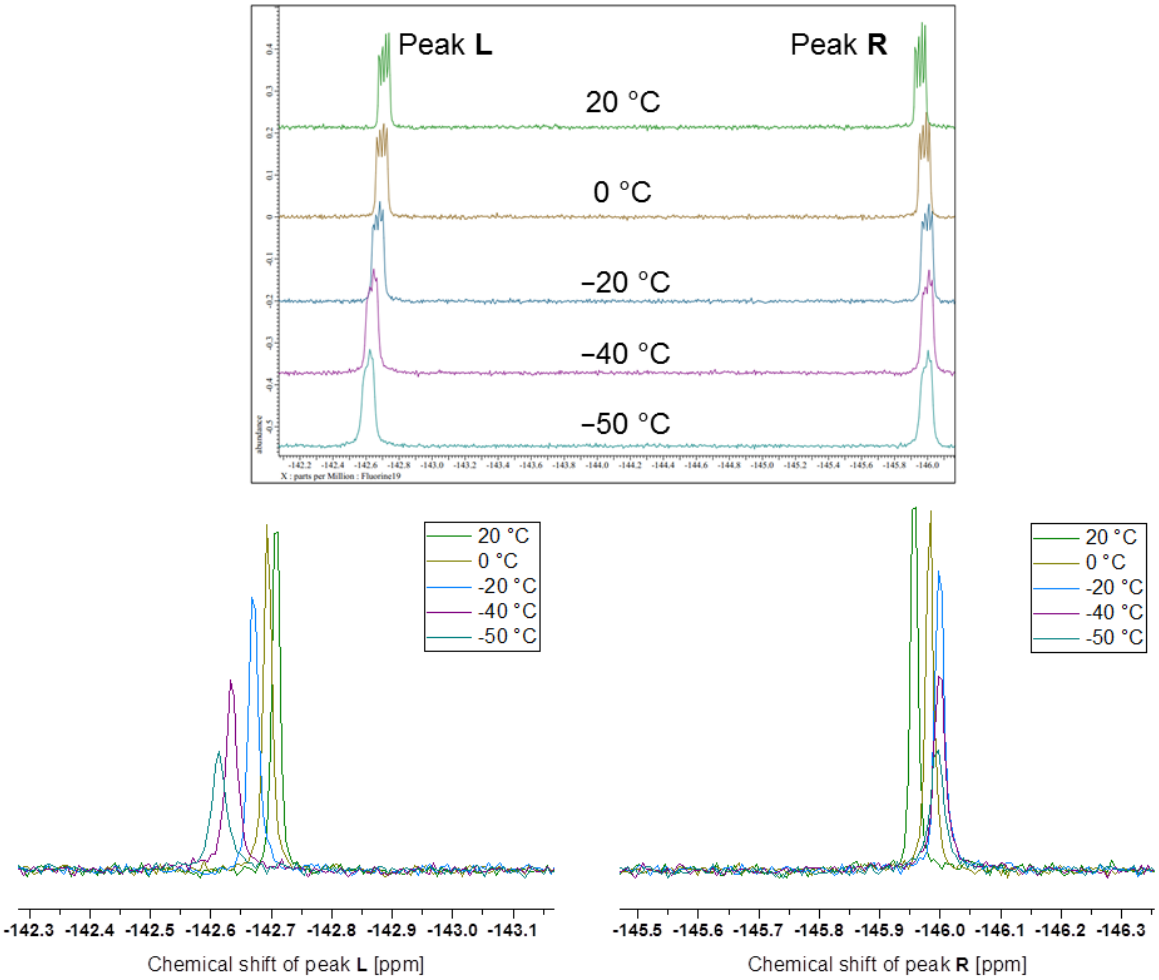

Figure 10. Variable temperature ^{19}F spectrum of compound **2**: comparison of spectra with the lowering of the temperature (top), and the shapes and positions of peaks L (bottom left) and R (bottom right) following decoupling.

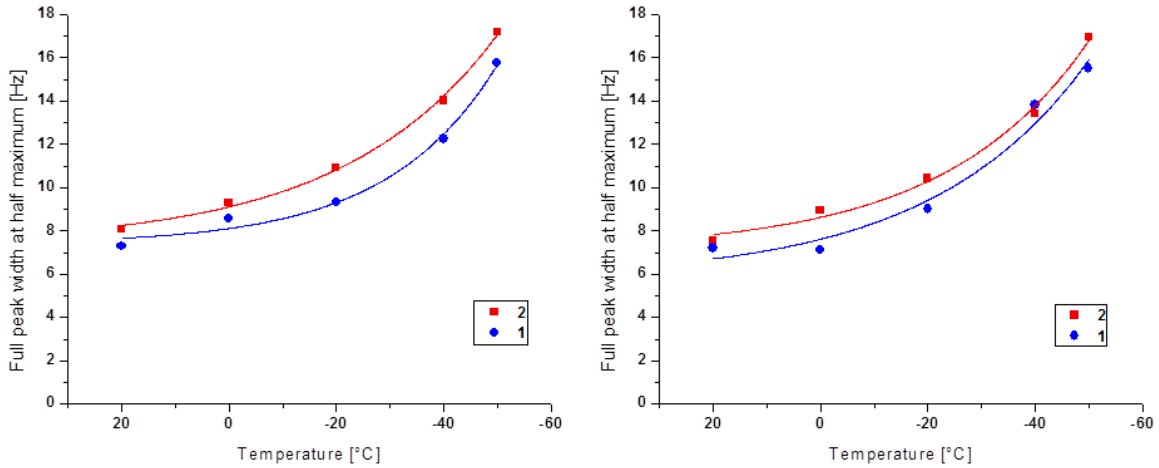

Figure 11. Comparison of full peak widths at half maximum in Hz for peaks **L** (left) and **R** (right) in compounds **1** and **2**.

References

[1] T. Chen, I. Popov, W. Kaveevivitchai, Y. Chuang, Y. Chen, O. Daugulis, A. J. Jacobson and O. Š. Miljanić, *Nat. Commun.*, 2014, **5**, doi: 10.1038/ncomms6131.

[2] V. I. Krasnov and V. E. Platonov, *Russ. J. Org. Chem.*, 1993, **29**, 895–896.